



HHS Public Access

Author manuscript

Nat Cell Biol. Author manuscript; available in PMC 2012 February 01.

Published in final edited form as:

Nat Cell Biol. ; 13(8): 958–965. doi:10.1038/ncb2286.

***MiR-193b-365*, a brown fat enriched microRNA cluster, is essential for brown fat differentiation**

Lei Sun^{1,8}, Huangming Xie^{1,3,6,8}, Marcelo A Mori⁵, Ryan Alexander^{1,7}, Bingbing Yuan¹, Shilpa M. Hattangadi^{1,4}, Qingqing Liu¹, C. Ronald Kahn⁵, and Harvey F. Lodish^{1,2,7,9}

¹ Whitehead Institute for Biomedical Research, 9 Cambridge Center, Cambridge, MA 02142, USA

² Department of Biological Engineering, Massachusetts Institute of Technology, Cambridge, MA 02139, USA

³ Computation and Systems Biology, Singapore-MIT Alliance, National University of Singapore, 4 Engineering Drive 3, Singapore 117576

⁴ Department of Hematology, Boston Children's Hospital, Boston, MA 02115

⁵ Section on Integrative Physiology and Metabolism, Research Division, Joslin Diabetes Center, Harvard Medical School, Boston, Massachusetts, USA

⁷ Department of Biology, Massachusetts Institute of Technology, Cambridge, MA 02139, USA

Abstract

Mammals have two principal types of fat. White adipose tissue (WAT) primarily serves to store extra energy as triglycerides, while brown adipose tissue (BAT) is specialized to burn lipids for heat generation and energy expenditure as a defense against cold and obesity^{1, 2}. Recent studies demonstrate that brown adipocytes arise *in vivo* from a *Myf5*-positive, myoblastic progenitor by the action of *Prdm16* (PR domain containing 16). Here, we identified a brown fat-enriched miRNA cluster, *miR-193b-365*, as a key regulator of brown fat development. Blocking *miR-193b* and/or *miR-365* in primary brown preadipocytes dramatically impaired brown adipocyte adipogenesis by enhancing *Runx1t1* (runt-related transcription factor 1; translocated to, 1) expression whereas myogenic markers were significantly induced. Forced expression of *miR-193b* and/or *miR-365* in C2C12 myoblasts blocked the entire program of myogenesis, and, in adipogenic condition, *miR-193b* induced myoblasts to differentiate into brown adipocytes.

Users may view, print, copy, download and text and data- mine the content in such documents, for the purposes of academic research, subject always to the full Conditions of use: http://www.nature.com/authors/editorial_policies/license.html#terms

⁹Correspondence: Whitehead Institute for Biomedical Research, 9 Cambridge Center, Cambridge, MA 02142, USA; Tel: 617 258 5216; Fax: 617 258 6768; lodish@wi.mit.edu.

⁶Present address: Division of Newborn Medicine, Department of Medicine, Children's Hospital Boston, 300 Longwood Avenue, Boston, MA 02115, USA

⁸These authors contributed equally to this work.

AUTHOR CONTRIBUTIONS

L.S, H.X and H.F.L conceived the project and designed the experiments. L.S, H.X, M.A.M, R.A, B.Y, S.M.H and Q.L performed the experiments. All authors analyzed data. L.S, H.X, M.A.M, H.F.L wrote the manuscript. C.R.K and H.F.L supervised the project.

COMPETING FINANCIAL INTERESTS

The authors declare no financial conflict of interest.

Accession number:

E-MEXP-2553; GSE27614

MiR-193b-365 was upregulated by *Prdm16* partially through *Ppara*. Our results demonstrate that *miR-193b-365* serves as an essential regulator for brown fat differentiation, in part by repressing myogenesis.

Keywords

miR-193; *miR-365*; *miR-193b-365*; microRNA; brown fat; brown adipocyte; lineage determination; adipogenesis; myogenesis; *Prdm16*

Although the amount of BAT in human adults was previously thought to be minimal, recent studies demonstrated that adult humans have substantial amounts of functioning BAT³⁻⁵, which inversely correlates with BMI and positively correlates with resting metabolic rate³. Loss of BAT activity may contribute to obesity and development of insulin resistance. When BAT is genetically or surgically ablated, mice develop hyperphagia and obesity⁶⁻⁸. Mice deficient of *Ucp1* (Uncoupling Protein 1), the hallmark of brown fat, are more susceptible to diet-induced obesity and develop obesity at thermoneutrality even when they are fed a control diet⁹. Conversely, expression of *Ucp1* in white adipocytes promotes energy expenditure and prevents the development of dietary and genetic obesity^{10, 11}. In addition, Bartelt. *et al.* demonstrated that brown fat is a major organ for triglyceride clearance¹². Therefore, understanding the mechanisms controlling the development of BAT may provide new therapeutic strategies for obesity and related disorders. Although, for decades, it was believed that brown adipocytes and white adipocytes share a common progenitor, a lineage tracing study demonstrated that brown adipocytes arise from a *Myf5*-positive, myoblastic lineage¹³. *Prdm16* is a key regulator that controls the switch between brown fat and muscle lineage. Ectopic expression of *Prdm16* together with *CEBPβ* can induce a functional BAT program in myoblasts and skin fibroblasts¹⁴. Knockdown of *Prdm16* in brown preadipocytes causes an induction of skeletal myogenesis¹³. However, other factors that regulate the switch between BAT and skeletal muscle remain unknown. Here, we show that the *miR-193b-365* cluster is important for lineage determination of brown adipocytes.

To uncover miRNAs that are important for brown fat lineage determination, we first identified lineage-enriched miRNAs by comparing the genome-wide miRNA expression patterns of mouse epididymal WAT, interscapular BAT and skeletal muscle using miRNA microarrays. Based on the criteria described in Methods, 91 miRNAs were expressed in at least one sample and differentially expressed between the three tissues (Fig. 1a and Fig. S1a). Among BAT-enriched miRNAs, *miR-193b* and *miR-365* were particularly interesting, since they are co-located on chromosome 16 as a ~5kb cluster (Fig. S1b), suggesting that they are a bicistronic transcript.

Cap-analysis gene expression (CAGE) Basic and Analysis Databases store original results produced by CAGE-seq which measures expression levels of transcription starting sites by sequencing large numbers of 5' transcript ends, termed CAGE tags^{15, 16}. We examined the distribution of CAGE tags surrounding the *miR-193b* and *miR-365-1* genes, and found that there was no CAGE tag between *miR-193b* and *miR-365-1* in the direction of transcription (Fig. S1b). Furthermore, we designed 14 pairs of primers across the genomic region of *miR-193b-365*, and performed RT-PCR to detect the primary transcripts of overlapping

segments of the *miR-193b-365* gene (Supplementary Fig. S1c). The amplified fragments covered the entire region between *miR-193b* and *miR-365*. Together, these data strongly suggest that *miR-193b-365* is a co-transcribed miRNA cluster.

We performed real-time PCR to examine the expression of *miR-193b* and *miR-365* in 14 adult mouse tissues (Fig. 1b); both miRNAs were enriched in BAT. We measured their expression levels at different time points during brown adipocyte differentiation of stromal-vascular fraction (SVF) cells from interscapular brown fat (Fig. 1c). Both miRNAs showed significant up-regulation during adipogenesis, ~5-fold for *miR-193b* and ~4-fold for *miR-365*. Furthermore, the levels of these two miRNAs were reduced by ~30% in brown fat of *ob/ob* mice, animals in which brown fat activity was impaired (Fig. S1d)¹⁷. Their levels in BAT were not changed in animals that were exposed to cold temperature (Fig. S1e) or in cell cultures that were treated with cAMP to induce the thermogenesis program (Fig. S1f).

To determine the functions of *miR-193b* and *miR-365* in brown adipocytes, we transfected brown fat SVF cells with locked nucleic acid (LNA) miRNA inhibitors and induced them to differentiate for 4 days. Since *miR-193a* shares the same seed sequence with *miR-193b*, the effects of a *miR-193a* inhibitor was also examined. For each inhibitor, RT-PCR detected a greater than 90% decrease of corresponding miRNA levels (Fig. 2a), which reflects a degradation or sequestration of miRNAs by inhibitors. Next, we performed mRNA microarray analysis to test whether knockdown of miRNAs caused global up-regulation of their targets. As predicted by TargetScanv5.1¹⁸, 559 and 513 messages are predicted targets of *miR-193a/b* and *miR-365* (context score < -0.2) respectively; 469 and 404, respectively, were expressed above background in our array data. The relative expression of each gene was calculated as a ratio of expression in knockdown vs. control cells, and the cumulative fraction was plotted as a function of the relative expression. The cumulative curve of the miRNA target genes shifted significantly to the right relative to the curve of the control genes that comprise genes without predicted miRNA target sites (Fig. 2b), indicating that miRNA targets, as a group, tended to be upregulated upon miRNA inhibitor transfection. Thus we conclude that these inhibitors functionally block downregulation of target miRNAs in cells. Note that both *miR-193a* and *miR-193b* inhibitors caused upregulation of *miR-193a/b*-targeted mRNAs, suggesting that either inhibitor was sufficient to suppress this miRNA family.

Blocking *miR-193a/b* and/or *miR-365* but not the control miRNA caused a remarkable reduction in lipid accumulation in brown adipocytes differentiated from SVF cells and brown preadipocytes (*Sca-1*⁺/*CD45*⁻/*CD11b*⁻) purified as described by Tseng laboratory¹⁹ (Fig. 2c, Fig. S2a,b,c). A substantial fraction of transfected cells had a fibroblast-like appearance (Fig. S2d). These effects of the inhibitors could be reversed by co-transfection with miRNA mimics of *miR-193a*, *miR-193b*, and *miR-365* (Fig. 2d), establishing the specificity of miRNA knockdown. As assayed by real-time PCR, cells transfected with miRNA inhibitors displayed marked down-regulation of adipogenesis markers common in brown and white fat including *AdipoQ*, *Cebpa*, *Fabp4* and *Pparγ* (Fig. 2e, Fig. S2c). A more dramatic decrease was observed in expression of several brown fat enriched markers – *Ucp1*, *Pparα*, *Pgc-1α*, *Dio2*, *Prdm16* and *Cidea* (Fig. 2f, g, Fig. S2c). The reduction of *Ucp1* expression was confirmed by Western blotting (Fig. 2g, Fig. S2e). However, the

expression of these genes was not altered in mature brown adipocytes transfected with miRNA inhibitors (Fig. S2f), suggesting that these miRNAs perform their primary functions during development and not in mature adipocytes. In addition, miR-193a/b and *miR-365* were also required for white fat adipogenesis (Fig. S2h, i), indicating that they were general regulators of adipogenesis with an additional role in supporting the development of brown fat cells.

Among the conserved targets predicted by TargetScanv5.1, *Runx1t1* is one of the top candidates of miR-193b. *Runx1t1* inhibits brown fat adipogenesis (Fig. S3a-e) and, as reported previously, inhibits white adipogenesis in 3T3-L1 cells²⁰⁻²². Upon blocking *miR-193a/b*, *Runx1t1* was upregulated at both the messenger RNA (Fig. 2h) and the protein levels (Fig. S3f). To prove that *miR-193b* can directly target *Runx1t1* mRNA, we cloned the 3'UTR segment of *Runx1t1* containing the predicted *miR-193b* target site (or a mutated seed site) into the psiCHECK-2 vector. Each of the reporter constructs was co-transfected with *miR-193b* mimic into 293T cells. Luciferase reporter assay showed that *miR-193b* mimic reduced the activity of the reporter with a wild-type 3'UTR but not the one with mutations in the seed sequences (3'UTR_Mut) (Fig 2. i). This demonstrates that *miR-193b* directly interacts with the predicted target sites in the *Runx1t1* mRNA, and the downregulation of *Runx1t1* partially explains the role of *miR-193b* during adipogenesis.

Because previous studies have shown that brown fat and skeletal muscle share a common developmental origin^{13, 14}, we suspected that blockage of the brown adipocyte lineage by knockdown of *miR-193b* and/or *miR-365* might switch the fate of brown preadipocytes to the muscle lineage. Indeed, RT-PCR analysis showed that expression of several myogenic markers (*Ckm*, *Myf5*, *Myf6*, *Myod* and *Myog*) was significantly induced (Fig. 3a), indicating a tendency towards myogenesis in the inhibitor-transfected brown preadipocytes.

The induction of myogenesis in brown adipocytes could be a direct effect of blocking *miR-193b* and/or *miR-365*, or secondary to the inhibition of brown adipogenesis as muscle markers are downregulated during brown fat differentiation²³. To further distinguish among these possibilities, we used retroviral vectors to express *miR-193b* and/or *miR-365* in C2C12 myoblasts which were subsequently induced to differentiate. At day 6, C2C12 cells expressing the control virus differentiated into elongated multinucleated myotube syncytia, whereas cells expressing *miR-193b* and/or *miR-365* failed to differentiate (Fig. 3b, Fig. S4a). Similar results were observed when miR-193a was ectopically expressed (Fig. S4b, c, d). Real-time PCR (Fig. 3d) and Western blot (Fig. 3c, Fig. S4e) analyses confirmed that ectopic expression of either miRNA decreased the mRNA levels of the myogenic markers *Myf5*, *Myf6*, *Myog*, *Ckm*, *Tnni2*, *Tnnt3* and *Casq1*, as well as the level of myosin protein. This analysis thus demonstrates that *miR-193b-365* can directly repress myogenesis, thereby contributing to the regulation of brown fat *versus* muscle lineage determination.

Among the conserved targets predicted by TargetScanv5.1 are *Cdon* (also named *Cdo*) and *Igfbp5*, both previously implicated as pro-myogenic factors. *Cdon* is a cell surface receptor that stimulates post-translational activation of myogenic bHLH factors and E proteins, and increases muscle-specific transcription^{24, 25, 26}. Knocking down *Igfbp5* also impairs myogenic differentiation of C2C12 and primary skeletal muscle cells²⁷. Real-time PCR and

Western blot analysis showed that the levels of both *Cdon* and *Igfbp5* mRNAs and protein were significantly reduced in C2C12 cells expressing *miR-193b* (Fig. 3e,f, Fig. S4f). We also examined their expression in cultured brown adipocytes transfected with LNA-193a/b inhibitors, and found that their expression was upregulated (Fig. 3g). To further establish that *miR-193b* directly down-regulates *Cdon* and *Igfbp5* expression, we performed luciferase reporter assay as we did for *Runx1t1*. As we expected, *miR-193b* mimic reduces the activities of both *Cdon* and *Igfbp5* reporters with a wild-type 3'UTR but not reporters with mutations in the seed sequences in the 3'UTRs (3'UTR_Muts) (Fig 3h). This demonstrates that *miR-193b* directly interacts with both predicted target sites.

Not only did ectopic expression of *miR-193b* repress myogenesis by C2C12 myoblasts, it also upregulated the mRNAs encoding two master adipogenic factors *Ppar γ* and *Cebpa* by ~10 fold and ~2.5 fold respectively (Fig. S5a). Furthermore, when exposed to pro-adipogenic differentiation conditions (detailed in Methods), C2C12 cells expressing *miR-193b* showed a round, lipid droplet-containing appearance, which resembled the morphology of adipocytes (Fig. 4a). Ectopic expression of *miR-193b* repressed the expression of myogenic markers *Pax3* and *MyoD* (Fig. 4b, Fig. S5c) while it promoted a significant upregulation of the common adipogenesis markers *AdipoQ*, *Ppar γ* , *Cebpa* and *Fabp4* as well as brown fat selective markers, *Ucp1*, *Cidea*, *Prdm16* and *Ppara* (Fig. 4b, c). Strikingly, the expression of markers such as *AdipoQ*, *Cebpa*, *Ppar γ* and *Fabp4* was comparable to their levels in cultured brown adipocytes (Fig S5b). The *miR-193b*-induced adipocytes also displayed an oxygen consumption rate (ORC) profile characteristic of brown adipocytes. Although ORC for basal respiration, non-mitochondrial respiration, and respiration capacity were not changed by *miR-193b* expression, a significantly higher ORC for proton leakage and a lower ORC for ATP turnover were observed in *miR-193b*-induced adipocytes (Fig. 4e). *Bona fide* brown adipocytes should initiate a thermogenesis program in response to beta-adrenergic stimulation, which can be mimicked by cAMP treatment. In response to cAMP treatment, the thermogenic makers, *Ucp1* and *Pgc-1a*, were upregulated by ~15- and ~5-fold respectively in *miR-193b*-expressing C2C12 cells (Fig. 4d). Thus, *miR-193b* can induce brown fat adipogenesis in C2C12 myoblast cells.

C2C12 myoblasts are known to be able to differentiate into adipocytes²⁸. To exclude the possibility that the adipogenesis of C2C12 cells is due to effects of their transformation, and also to test whether the effects of *miR-193b* on myoblasts are conserved between mouse and human, we retrovirally expressed *miR-193b* in primary human myoblasts which were subsequently exposed to myogenic or adipogenic differentiation conditions (detailed in Methods). *MiR-193b*, but not *miR-365* (data not shown), significantly repressed myogenesis (Fig S5d, e, f) and promoted the expression of all 5 adipogenic markers we examined (*Fabp4*, *AipoQ*, *Cebpa*, *Lpl*, *Pparg*) (Fig S5g). Together, our studies establish that *miR-193b*'s functions in repressing myogenesis and promoting adipogenesis are conserved between mouse and human.

Prdm16 has been reported to be the “master” regulator of BAT lineage determination^{13, 14, 29, 30}. To determine whether induction of *miR-193b-365* is part of the *Prdm16*-induced program, we used retroviral vectors to introduce *Prdm16* into subcutaneous primary white preadipocytes and C2C12 myoblasts. By day 6 of differentiation, both

miR-193b and *miR365* were significantly upregulated in cells ectopically expressing *Prdm16* (Fig. 5a, Fig. S6a, b). Conversely, retroviral shRNA knockdown of *Prdm16* in brown adipocyte cultures resulted in ~75% decrease in *miR-193b* expression and ~50% decrease in *miR-365* expression (Fig. 5b). Thus, *miR-193b-365* is regulated by *Prdm16*.

Sequence analysis of the promoter region of *miR-193b-365* by Explain 3.0 of BIOBASE predicted three *Ppara/RXR* binding sites within the 1 KB segment upstream of *miR-193b* (Fig. 5e). *Ppara* is a brown fat-selective transcriptional factor and is important for fatty acid oxidation^{31, 32} and suppressing expression of muscle-associated proteins in brown adipose tissue³³. Interestingly, the expression of *Ppara* could be induced by ectopic expression of *Prdm16* in primary white preadipocytes (Fig. S6a) and *Ppar γ* -deficient mouse embryonic fibroblasts²⁹. *Ppara* can also directly interact with *Prdm16*¹³. Thus, we hypothesized that *Prdm16* might regulate *miR-193b-365* through *Ppara*. To test this hypothesis, we knocked down *Prdm16* in primary brown adipocyte cultures, which resulted in about 80% decrease of *Ppara* mRNA (Fig. 5c). Consistently, the induction of *Prdm16* and *Ppara* was slightly prior to the induction of *miR-193b-365* during brown fat adipogenesis (Fig. 5d). A direct interaction between *Ppara* and the promoter region of *miR-193b-365* was confirmed by chromatin immunoprecipitation (ChIP) (Fig. 5e). In addition, a moderate but statistically significant down-regulation of *miR-193b* and *miR-365* was observed in primary brown adipocyte cultures transfected with *Ppara* siRNA (Fig. 5f) and in brown adipose tissues from *Ppara* knockout compared to wild-type mice (Fig. 5g). To rigorously prove that *Prdm16*-*Ppara* regulates *miR-193b-365* at the transcriptional level, we used Real-time PCR to examine the levels of pri-*miR-193b-365* and found that the pri-miRNA was regulated similarly as mature *miR-193b* and *miR-365* by *Prdm16* and *Ppara* (Fig. S6c-h). Together, these data suggest that *Prdm16* can induce *miR-193b-365* expression at least partially by inducing expression of *Ppara*.

Since ectopic expression of *miR-193b* promotes the expression of *Prdm16* (Fig. 4c) and since blocking *miR-193b* in brown preadipocytes results in a down-regulation of *Prdm16* (Fig. 2f), we hypothesize a feed-forward loop that ensures differentiation of brown adipocytes from bipotential brown adipocyte/myocyte progenitors (Fig S6m). To test whether the effects of *miR-193b* on brown fat adipogenesis can be solely attributed to its effects on *Prdm16*, we blocked *miR-193b-365* in brown adipocyte cultures ectopically expressing *Prdm16*. Overexpression of *Prdm16* in brown preadipocytes was not sufficient to fully rescue the deficiency in adipogenesis due to a blockage of *miR-193a/b* or *miR-365* (Fig. S6i-l). Thus, *miR-193b* likely regulates more factors additional to *Prdm16* to control brown fat adipogenesis.

To the best of our knowledge, the present work is the first study to investigate the functions of miRNA in brown fat specification, and our results have revealed another layer of regulation of brown fat lineage determination. Further functional characterization of *miR-193b* and *miR-365* in animal models and better understanding of the mechanisms regulating brown fat development may lead to identification of novel therapeutic targets and strategies against obesity and related metabolic disorders.

METHODS

Cell cultures

Primary brown adipocytes and SVF cells were fractionated and cultured according to published methods with few modifications^{34, 35}. Briefly, 2 week old C57BL/6 mice were sacrificed. Interscapular BAT were harvested and digested with collagenase (0.2%). SVF cells were collected by centrifugation, red blood cells were lysated with NH₄Cl and then SVF were filtered through 40uM. Primary white SVF cells and adipocytes from subcutaneous fat were isolated and fractionated according to published methods³⁶. Primary SVF cells were cultured to confluence in DMEM with 10% New Born Calf Serum (Invitrogen) and induced to differentiate for 2 days with DMEM containing 10%FBS DMEM, Insulin 850nM (Sigma), Dexamethasone 0.5uM (Sigma), IBMX 250uM (Sigma), Rosiglitazone 1uM (Cayman Chemical), T3 1nM (Sigma), and Indomethacin 125nM (Sigma). The induction medium was replaced with DMEM containing 10% FBS and 160nM insulin for 2 day. Then cells were incubated in DMEM with 10% FBS.

The immortalized brown adipocyte cell line used for ChIP was a generous gift from the Dr. Ronald Kahn lab. Cells were cultured to confluence then exposed to differentiation media: 10%FBS DMEM, Insulin 20nM (Sigma), Dexamethasone 0.5uM (Sigma), IBMX 250uM (Sigma), T3 1nM (Sigma), and Indomethacin 125nM (Sigma) for 2 days. Cells were then switched to media containing 10%FBS, T3 (1nM) and Insulin (20nM).

C2C12 and HEK 293T cells from the American Type Culture Collection (ATCC) were cultured or differentiated according to manufacturer's instructions.

Primary human myoblasts were purchased from ZenBio. Cells were cultured and differentiated according to manufacturer's instructions.

Animal studies

Male C57BL/6J mice, Ppar α knockout mice (B6:129S4) and ob/ob mice (000632) from the Jackson Laboratory were maintained at the animal facility of the Whitehead Institute for Biomedical Research. All animal experiments were performed with the approval of the Massachusetts Institute of Technology Committee on Animal Care. Epididymal WAT, interscapular BAT and skeletal muscle from 12 week old mice were harvested after perfusion for miRNA expression profiling and RT-PCR. Tissues from 4–5 mice were pooled for each RNA sample preparation. Brown fat of Ppar α knockout mice was harvested from 8 weeks old mice (male), and age-matched wild-type mice were used as a control. 8 week old male C57BL/6 mice were kept in 4oC for 24 hours to stimulate brown fat thermogenesis.

Plasmids and Viral Vectors

Authentic miRNA stem-loop and ~ 220 nucleotide flanking sequences on the 5' and 3' side of the mmu-miR-193a/b and mmu-*miR-365-1* gene were amplified from normal mouse genomic DNA (Clontech) and cloned into a retroviral vector containing IRES-GFP as described previously³⁷ for retrovirus production. The *Prdm16* retroviral construct (15504), *Prdm16*-shRNA retroviral construct (15505), and Pparg2 retroviral construct (8859) were

purchased from Addgene. Runx1t1 and its GFP vector control constructs are generous gift from Rochford's lab. Retroviral package vectors pcl-ECO and pcl-10A1 are from IMGENEX.

To generate reporter constructs for luciferase assays, about 400 bp segments containing predicted miRNA target sites in the 3'UTRs of *Runx1t1*, *Cdon* and *Igfbp5* were cloned into the psiCHECK-2 vector (Promega) between the XhoI and NotI sites immediately downstream of the *Renilla* luciferase gene. To generate reporters with mutant 3'UTRs, five nucleotides (CCAGT) in the target site complementary to the position 2–6 of *miR-193b* seed region were mutated to GATCC by a QuikChange Site-Directed Mutagenesis kit according to the manufacturer's protocol (Stratagene).

Induction of brown fat adipogenesis in myoblasts

To induce *miR-193b*-expressing myoblasts for adipogenesis, C2C12 myoblasts or primary human myoblasts were infected as described below, cultured to confluence, and then exposed to brown adipocyte differentiation conditions: 10%FBS DMEM, Insulin 850nM (Sigma), Dexamethasone 0.5uM (Sigma), IBMX 250uM (Sigma), Rosiglitazone 1uM (Cayman Chemical), T3 1nM (Sigma), and Indomethacin 125nM (Sigma). After 2 days, cells were incubated in culture medium containing insulin 160nM and Rosiglitazone 1uM for another 2 days, and then were switched to 10% FBS DMEM. To stimulate thermogenesis, cells were incubated with dibutyryl cAMP 0.5mM (Sigma) for 4 h.

FACS sorting

Brown fat SVF cells were isolated as described above. SVF cells were stained with a FITC-conjugated CD45 antibody (Ebioscience), APC-conjugated CD11b (Ebioscience) antibody and PE-conjugated Sca1 antibody (Ebioscience) for 15 mins on ice. Cells were washed twice and then resuspended in PBS (2% FBS, PI). FACS sorting was performed at Whitehead Institute core facility to enriched CD45⁻ CD11b⁻ Sca1⁺ preadipocytes.

Retrovirus production and Infection

Empty vector or expression plasmid (8 µg) was co-transfected with retrovirus packaging vector pCL-Eco (4 µg) into 80% confluent 293T cells (100mm plate) using FuGene 6 according to the manufacturer's protocol (Roche). Virus supernatant was collected 2 days after transfection.

Primary white and brown fat SVF cells and C2C12 myoblasts were cultured to 30–50% confluence and infected with retrovirus in the presence of 4 µg/ml polybrene (Sigma). Infection efficiency was generally higher than 80%, as judged by GFP expression when viewed under the microscope or by FACS analysis.

Luciferase Reporter assay

293T cells were seeded in 96-well white assay plates (Corning) at a density of 30,000 cells per well one day before transfection. Ten nanograms of each reporter construct were co-transfected with *miR-193b* mimic or a mimic control (Dharmacon) at final concentration 50nM into 293T cells using Lipofectamine 2000 according to the manufacturer's protocol

(Invitrogen). After 48 hours, firefly and *Renilla* luciferase activities were measured with the Dual-Glo luciferase assay system according to the manufacturer's instructions (Promega).

Transfection of LNA miRNA inhibitor and siRNAs

When cultured SVF cells or sorted preadipocytes were grown to 70–80% confluence, Locked Nucleic Acids (LNAs) miRNA inhibitors (100nM) or anti-Ppara siRNA (200nM) were transfected by DharmaFect 2 (6ul/ml) according to the manufacturer's instruction. 24 hrs after transfection, cells were recovered in full culture media and grown to confluence for differentiation. LNAs inhibitors were from Exiqon, LNA-193b (139676-00), LNA-365 (139215-00), LNA-193 (139481-00) and LNA-Ctl (199002-08). siRNAs for Ppara were from Invitrogen, MSS207857 and negative control (12935300)

miRNA microarray and data analysis

miRNA microarray and analysis were performed as previously described³⁸. Specifically, microarrays with miRNA content corresponding to miRBase v10.1 (six probes for each miRNA on one chip) were used. After global normalization, miRNAs with an intensity more than 500 arbitrary units were considered as expressed. Differentially regulated miRNAs were identified by one-way ANOVA analysis ($P < 0.1$). 91 miRNAs expressed in at least one sample and differentially expressed between three tissues were selected for clustering analysis. Unsupervised hierarchical clustering was performed with average linkage and uncentered correlation as the similarity metric using Cluster3.0³⁹. The heat map was generated in Java Treeview. Accession number: E-MEXP-2553 (ArrayExpress).

mRNA microarray and data analysis

Total mRNA was obtained from primary brown adipocytes transfected with miRNA inhibitor or Control inhibitor. Affymetrix arrays were performed by the Genome Technology Core at Whitehead Institute. Microarray data were preprocessed with RMA from the Affymetrix package in Bioconductor using custom probeset definitions for NCBI Entrez Genes derived from previous method⁴⁰. To reduce data noise, genes with intensities below threshold ($\log_2(\text{Value}) < 3$, arbitrary units) were removed from further analysis. TargetScan v5.1¹⁸ was used for predicting miRNA targets. Relative expression of each gene was calculated as the \log_2 ratio between the intensity of the mRNA in the miRNA inhibitor sample relative to the intensity of the control inhibitor sample. The cumulative fraction was plotted as a function of the relative expression. The cumulative curves for both miRNA targets and the genes without miRNA binding sites were plotted, and one-sided Kolmogorov-Smirnov test was performed as the statistical test. mRNA microarray data have been uploaded to GEO GSE27614.

Quantitative real-time PCR assay and Western blot

RT PCR for miRNA and mRNA was performed and analyzed as previously described³⁸. Primer sequences are listed in Supplementary Table SI. 18S was used as an internal control.

For Western blot analyses, cells or tissues were lysed in RIPA buffer (0.5% NP-40, 0.1% SDS, 150 mM NaCl, 50 mM Tris-Cl (pH 7.5)). Proteins were separated by SDS-PAGE, transferred to Nitrocellulose membrane (Millipore) and probed with anti-Cdon (AF2429,

R&D system), anti-Igfbp5 (AF578, R&D system), Anti-*Ucp1* (ab10983, Abcam), anti-MyoD (SC-760, Santa Cruz), anti-PAX3 (ab15717, Abcam), anti-Runx1t1 (SC-9737, Santa Cruz), and anti-Myosin (MF20, Developmental Studies Hybridoma Bank) antibodies.

Chromatin immunoprecipitation

Immortalized brown fat cell culture cells (3×10^7 cells per sample) were fixed with formaldehyde at 1% final concentration for 20 minutes. The cross-linking was quenched with ice-cold 2.5M glycine, and the cells were rinsed twice with 1x PBS. Cross-linked cells were resuspended, then lysed with detergent to separate the nuclear pellet which was resuspended in 3ml sonication buffer (50mM Tris HCl, 140mM NaCl, 1mM EDTA, 1% Triton-X 100, 0.1% Na-deoxycholate, 0.1% SDS), and then sonicated to shear the cross-linked DNA to an optimal fragment size ranging from 200 to 500 bp. Sonication was performed using a Branson sonifier (at Power 4.5 for 24W at maximum power) for nine 20-second pulses (with a 60-second pause between pulses). Simultaneously, magnetic protein-G beads (Dyna) were incubated with 20ug polyclonal antibody against Ppar α (SC-9000X, Santa Cruz) or 20ug IgG control (rat IgG #012-000-003 from Jackson) for 6 hours on ice. An aliquot (1/600) of the sonicated nuclear pellet was set aside as the whole cell extract control (WCE) and then taken through the rest of the protocol exactly as the immunoprecipitated (IP) fraction. The remainder (about 3ml) of the sonication sample was combined with the preincubated beads and this immunoprecipitation was run overnight at 4 degrees C. The beads were then collected with a magnet and washed with RIPA buffer 6 times. Bound DNA-protein complexes were eluted from the beads by reversal of cross-linking through heating to 65 degrees C overnight. The enriched IP and unenriched WCE DNA fragments were purified using RNase A and proteinase K incubation, phenol-chloroform extraction, and then ethanol precipitation. The resulting DNA was then used for gene-specific PCR.

Measurements of oxygen consumption and extracellular acidification rates

C2C12 cells were seeded (5,000 cells/well) into gelatin-coated XF24 V7 cell culture microplates (Seahorse Bioscience) and cultured overnight at 37°C with 5% CO₂. The next day, cells were transduced with retroviruses expressing *miR-193b* or empty vector in the presence of polybrene, cultured to confluence, and induced to differentiate with a brown adipocyte cocktail. As a control, primary brown preadipocytes were isolated, seeded into gelatin-coated XF24V7 cell culture microplates, and differentiated into mature brown adipocytes. At day 6 of differentiation, the media was replaced with prewarmed XF24 assay media for 1 h; this unbuffered media consisted of DMEM (Sigma), 1 mM Glutamax-1 (Invitrogen), 2 mM pyruvate, 141 mM NaCl, and 25 mM glucose. Using the Seahorse Bioscience XF24-3 Extracellular Flux Analyzer, the O₂ tension immediately around the cells was measured by optical fluorescent biosensors embedded in a sterile disposable cartridge placed into the wells of the microplate during the assay. O₂ consumption rate (OCR) was calculated by plotting the O₂ tension of the media in the microenvironment above the cells as a function of time (pmoles/min). OCR was measured during 4 min cycles repeated four times at 10-min intervals. Firstly, basal respiration was assessed in untreated cells. Secondly, ATP turnover was calculated in response to oligomycin (Calbiochem) treatment (10 μ M). Maximum respiratory capacity was assessed after FCCP (Sigma) stimulation (1 μ M).

Finally, mitochondrial respiration was blocked by Rotenone (Sigma) (1 μ M) and the residual OCR was considered non-mitochondrial respiration. Proton leak was calculated by subtracting the ATP turnover and the non-mitochondrial respiration components of basal respiration.

Statistical analysis

Data are expressed as means \pm SE unless otherwise indicated. Student's t test (unpaired, two-tailed) was used to compare the two groups, and the P value was calculated in Excel (Microsoft) or GraphPad Prism 5 (GraphPad Software). $P < 0.05$ was considered as statistically significant.

Supplementary Material

Refer to Web version on PubMed Central for supplementary material.

Acknowledgments

This work is supported by NIH grants DK047618, DK 068348, DK076848, and 5P01 HL066105, grant C-382-641-001-091 from the Singapore-MIT Alliance (SMA) and a graduate fellowship from SMA. Thanks for intellectual support, materials, and advice from members of the laboratories of Drs. Patrick Seale, David Bartel, Charles Emerson, and from all members of the Lodish laboratory. Thanks for Rochford's lab for their generous gifts of Runx1t1 plasmid.

References

1. Seale P, Kajimura S, Spiegelman BM. Transcriptional control of brown adipocyte development and physiological function--of mice and men. *Genes Dev.* 2009; 23:788–797. [PubMed: 19339685]
2. Gesta S, Tseng YH, Kahn CR. Developmental origin of fat: tracking obesity to its source. *Cell.* 2007; 131:242–256. [PubMed: 17956727]
3. Cypess AM, et al. Identification and importance of brown adipose tissue in adult humans. *N Engl J Med.* 2009; 360:1509–1517. [PubMed: 19357406]
4. van Marken Lichtenbelt WD, et al. Cold-activated brown adipose tissue in healthy men. *N Engl J Med.* 2009; 360:1500–1508. [PubMed: 19357405]
5. Virtanen KA, et al. Functional brown adipose tissue in healthy adults. *N Engl J Med.* 2009; 360:1518–1525. [PubMed: 19357407]
6. Connolly E, Morrissey RD, Carnie JA. The effect of interscapular brown adipose tissue removal on body-weight and cold response in the mouse. *Br J Nutr.* 1982; 47:653–658. [PubMed: 6282304]
7. Lowell BB, et al. Development of obesity in transgenic mice after genetic ablation of brown adipose tissue. *Nature.* 1993; 366:740–742. [PubMed: 8264795]
8. Hamann A, Flier JS, Lowell BB. Decreased brown fat markedly enhances susceptibility to diet-induced obesity, diabetes, and hyperlipidemia. *Endocrinology.* 1996; 137:21–29. [PubMed: 8536614]
9. Feldmann HM, Golozoubova V, Cannon B, Nedergaard J. *Ucp1* ablation induces obesity and abolishes diet-induced thermogenesis in mice exempt from thermal stress by living at thermoneutrality. *Cell Metab.* 2009; 9:203–209. [PubMed: 19187776]
10. Kopecky J, Clarke G, Enerback S, Spiegelman B, Kozak LP. Expression of the mitochondrial uncoupling protein gene from the aP2 gene promoter prevents genetic obesity. *J Clin Invest.* 1995; 96:2914–2923. [PubMed: 8675663]
11. Kopecky J, et al. Reduction of dietary obesity in aP2-Ucp transgenic mice: mechanism and adipose tissue morphology. *Am J Physiol.* 1996; 270:E776–786. [PubMed: 8967465]
12. Bartelt A, et al. Brown adipose tissue activity controls triglyceride clearance. *Nat Med.* 17:200–205. [PubMed: 21258337]

13. Seale P, et al. *Prdm16* controls a brown fat/skeletal muscle switch. *Nature*. 2008; 454:961–967. [PubMed: 18719582]
14. Kajimura S, et al. Initiation of myoblast to brown fat switch by a *Prdm16*-C/EBP-beta transcriptional complex. *Nature*. 2009; 460:1154–1158. [PubMed: 19641492]
15. Kawaji H, et al. CAGE Basic/Analysis Databases: the CAGE resource for comprehensive promoter analysis. *Nucleic Acids Res*. 2006; 34:D632–636. [PubMed: 16381948]
16. Carninci P, et al. The transcriptional landscape of the mammalian genome. *Science*. 2005; 309:1559–1563. [PubMed: 16141072]
17. Hogan S, Himms-Hagen J. Abnormal brown adipose tissue in obese (ob/ob) mice: response to acclimation to cold. *Am J Physiol*. 1980; 239:E301–E309. [PubMed: 7425122]
18. Friedman RC, Farh KK, Burge CB, Bartel DP. Most mammalian mRNAs are conserved targets of microRNAs. *Genome Res*. 2009; 19:92–105. [PubMed: 18955434]
19. Schulz TJ, et al. Identification of inducible brown adipocyte progenitors residing in skeletal muscle and white fat. *Proc Natl Acad Sci U S A*. 2010; 108:143–148. [PubMed: 21173238]
20. Payne VA, et al. C/EBP transcription factors regulate SREBP1c gene expression during adipogenesis. *Biochem J*. 2009; 425:215–223. [PubMed: 19811452]
21. Blumberg JM, et al. Complex role of the vitamin D receptor and its ligand in adipogenesis in 3T3-L1 cells. *J Biol Chem*. 2006; 281:11205–11213. [PubMed: 16467308]
22. Rochford JJ, et al. ETO/MTG8 is an inhibitor of C/EBPbeta activity and a regulator of early adipogenesis. *Mol Cell Biol*. 2004; 24:9863–9872. [PubMed: 15509789]
23. Timmons JA, et al. Myogenic gene expression signature establishes that brown and white adipocytes originate from distinct cell lineages. *Proc Natl Acad Sci U S A*. 2007; 104:4401–4406. [PubMed: 17360536]
24. Cole F, Zhang W, Geyra A, Kang JS, Krauss RS. Positive regulation of myogenic bHLH factors and skeletal muscle development by the cell surface receptor CDO. *Dev Cell*. 2004; 7:843–854. [PubMed: 15572127]
25. Kang JS, Mulieri PJ, Miller C, Sassoon DA, Krauss RS. CDO, a robo-related cell surface protein that mediates myogenic differentiation. *J Cell Biol*. 1998; 143:403–413. [PubMed: 9786951]
26. Kang JS, et al. A Cdo-Bnip-2-Cdc42 signaling pathway regulates p38alpha/beta MAPK activity and myogenic differentiation. *J Cell Biol*. 2008; 182:497–507. [PubMed: 18678706]
27. Ren H, Yin P, Duan C. IGFBP-5 regulates muscle cell differentiation by binding to IGF-II and switching on the IGF-II auto-regulation loop. *J Cell Biol*. 2008; 182:979–991. [PubMed: 18762576]
28. Teboul L, et al. Thiazolidinediones and fatty acids convert myogenic cells into adipose-like cells. *J Biol Chem*. 1995; 270:28183–28187. [PubMed: 7499310]
29. Seale P, et al. Transcriptional control of brown fat determination by *Prdm16*. *Cell Metab*. 2007; 6:38–54. [PubMed: 17618855]
30. Kajimura S, et al. Regulation of the brown and white fat gene programs through a *Prdm16*/CtBP transcriptional complex. *Genes Dev*. 2008; 22:1397–1409. [PubMed: 18483224]
31. Barbera MJ, et al. Peroxisome proliferator-activated receptor alpha activates transcription of the brown fat uncoupling protein-1 gene. A link between regulation of the thermogenic and lipid oxidation pathways in the brown fat cell. *J Biol Chem*. 2001; 276:1486–1493. [PubMed: 11050084]
32. Braissant O, Fougère F, Scotto C, Dauca M, Wahli W. Differential expression of peroxisome proliferator-activated receptors (PPARs): tissue distribution of PPAR-alpha, -beta, and -gamma in the adult rat. *Endocrinology*. 1996; 137:354–366. [PubMed: 8536636]
33. Tong Y, et al. Suppression of expression of muscle-associated proteins by PPARalpha in brown adipose tissue. *Biochem Biophys Res Commun*. 2005; 336:76–83. [PubMed: 16125138]
34. Cannon B, Nedergaard J. Cultures of adipose precursor cells from brown adipose tissue and of clonal brown-adipocyte-like cell lines. *Methods Mol Biol*. 2001; 155:213–224. [PubMed: 11293074]

35. Tseng YH, Ueki K, Kriauciunas KM, Kahn CR. Differential roles of insulin receptor substrates in the anti-apoptotic function of insulin-like growth factor-1 and insulin. *J Biol Chem.* 2002; 277:31601–31611. [PubMed: 12082100]
36. Rodbell M. Metabolism of Isolated Fat Cells. I. Effects of Hormones on Glucose Metabolism and Lipolysis. *J Biol Chem.* 1964; 239:375–380. [PubMed: 14169133]
37. Zhang J, Socolovsky M, Gross AW, Lodish HF. Role of Ras signaling in erythroid differentiation of mouse fetal liver cells: functional analysis by a flow cytometry-based novel culture system. *Blood.* 2003; 102:3938–3946. [PubMed: 12907435]
38. Xie H, Lim B, Lodish HF. MicroRNAs induced during adipogenesis that accelerate fat cell development are downregulated in obesity. *Diabetes.* 2009; 58:1050–1057. [PubMed: 19188425]
39. de Hoon MJ, Imoto S, Nolan J, Miyano S. Open source clustering software. *Bioinformatics.* 2004; 20:1453–1454. [PubMed: 14871861]
40. Dai M, et al. Evolving gene/transcript definitions significantly alter the interpretation of GeneChip data. *Nucleic Acids Res.* 2005; 33:e175. [PubMed: 16284200]

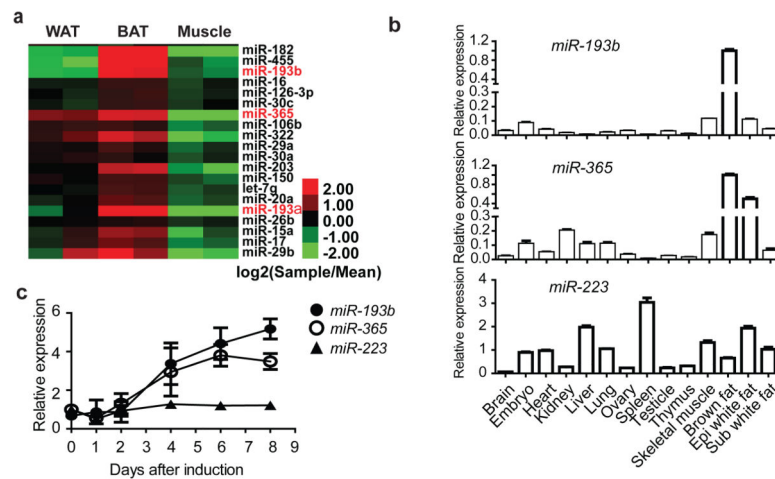


Figure 1. *miR-193b-365* is enriched in BAT

(a), Heat map showing the expression of miRNAs that are enriched in BAT compared to epididymal WAT and skeletal muscle. Red denotes higher and green denotes lower relative to the mean of the six samples for each miRNA. ($P < 0.1$, ANOVA). **(b)**, Real-time PCR analysis of *miR-193b*, *miR-365*, and a control miRNA, *miR-223* expression levels in BAT relative to other adult mouse tissues. $n=3$. **(c)**, Real-time PCR analysis of *miR-193b* and *miR-365* expression levels during adipogenesis of primary brown adipocyte cultures. $n=3$. Means \pm SEM.

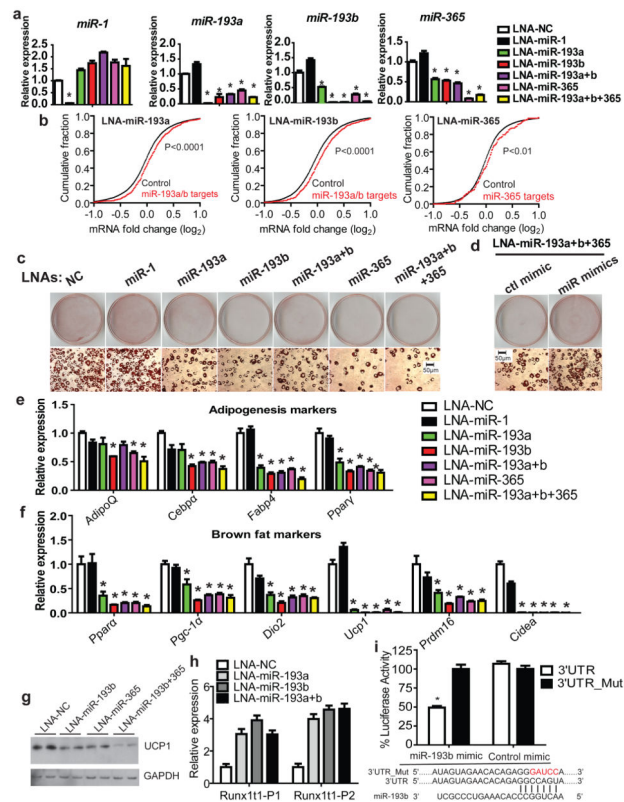


Figure 2. *miR-193b-365* is required for brown adipocyte adipogenesis

(a), SVF cells from brown fat were transfected with LNA miRNA inhibitors (100nM) one day before differentiation. RNAs were harvested at day 4. Real-time PCR was used to examine the expression of these miRNAs. $n=3$. (b), mRNAs from cultured primary brown adipocytes (Day 4) transfected with each inhibitor or Control inhibitor were analyzed by microarray analysis. On the x-axis is the relative expression of each gene calculated as a \log_2 ratio (x-axis) between its intensity in the miRNA-inhibited sample and its intensity in the control inhibitor sample. The cumulative fraction (y-axis) was plotted as a function of the relative expression (x-axis). “miRNA targets” (red line) represents the population of genes containing miRNA binding sites predicted by TargetScan, and “Control” (black line) represented all other genes lacking binding sites for the miRNA. The “targets” curve shifts to the right with a P value <0.05 as determined by the one-sided Kolmogorov-Smirnov test, indicating a trend of up-regulation of predicted targets in response to transfection of the miRNA inhibitor. (c), Oil red O staining was used to determine the accumulation of lipid droplets in brown adipocytes (Day 4). (d), SVF cells from brown fat were co-transfected with LNA miRNA inhibitors (100nM) and miRNA mimics (mimic-*miR-193a* 16.7nM, mimic-*miR-193b* 16.7nM and mimic-*miR-365* 16.7nM, or Control mimic 50nM) one day before differentiation. Four days after differentiation, ORO staining was used to determine lipid droplet content. (e), Real-time PCR analysis of the expression of adipogenesis markers and (f), Brown fat markers. $n=3$. (g), Western blot to examine the expression of *Ucp1*. (h), Effect of miR-193 knockdown on expression of *Runx1t1*. Real-time PCR was performed to examine the expression of *Runx1t1*. *Runx1t1*-P1 and *Runx1t1*-P2 represent two sets of PCR primers. $n=3$. (i), Luciferase reporter assay to examine the interactions between *miR-193b*

and the predicted target site in *Runx1t1* 3'UTR. Plasmids with the *Runx1t1* 3'UTRs or mutated UTRs were co-transfected with *miR-193b* mimic or a control mimic into 293T cells. Renilla luciferase activity was measured by Dual-Glo luciferase assay system and normalized to internal control firefly luciferase activity. n=6. * $P < 0.05$, Student's t-test; Means \pm SEM.

Author Manuscript

Author Manuscript

Author Manuscript

Author Manuscript

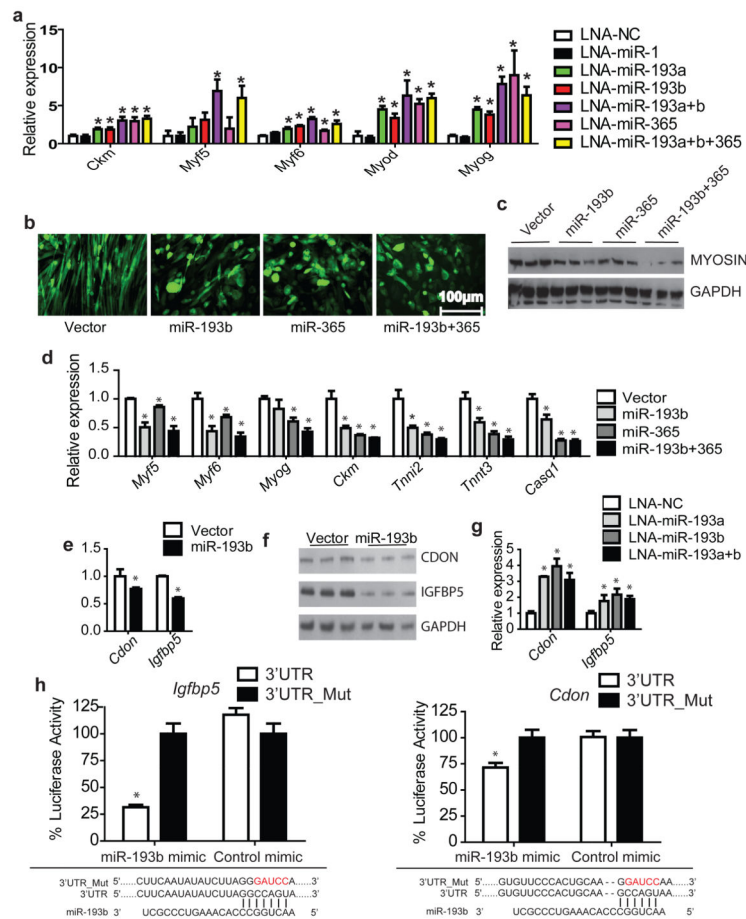


Figure 3. Ectopic expression of *miR-193b* and/or *miR-365* inhibits C2C12 myogenic differentiation

(a), SVF cells from brown fat were transfected with LNA miRNA inhibitors (100nM) one day before differentiation. At day 4, RNAs were extracted and Real-time PCR was performed to detect the expression of myogenic markers. $n=3$. (b), Representative micrographs of cells (Day 6 in 2% horse serum) differentiated from C2C12 myoblasts expressing retroviral *miR-193b* and/or *miR-365*, or control. GFP was expressed under control of an IRES downstream of the miRNA to visualize transfected cells. (c), Western blot with triplicate biological repeats to examine the expression of myosin upon ectopic expression of *miR-193b* and/or *miR-365*. (d), Real-time PCR analysis for expression of muscle markers. $n=3$. (e), Real-time PCR and (f), Western analysis for predicted *miR-193b* targets, cell adhesion molecule-related/down-regulated by oncogenes (*Cdon*) and insulin-like growth factor binding protein 5 (*Igfbp5*), in C2C12 cells expressing *miR-193b* or a control vector. $n=3$. (g), SVF cells from brown fat were transfected with LNA-*miR-193a* and/or LNA-*miR-193b*, and differentiated for 4 days. Real-time PCR was performed to examine the expression of *Cdon* and *Igfbp5*. $n=6$. (h), Luciferase reporter assay to examine the interactions between *miR-193b* and the predicted target site in *Cdon* and *Igfbp5* 3'UTR. Plasmids with the *Igfbp5* or *Cdon* 3'UTRs or mutated UTRs were co-transfected with *miR-193b* mimic or a control mimic into 293T cells. Renilla luciferase activity was

measured by Dual-Glo luciferase assay system, normalized to internal control firefly luciferase activity. n=6. * $P < 0.05$, Student's t-test; Means \pm SEM.

Author Manuscript

Author Manuscript

Author Manuscript

Author Manuscript

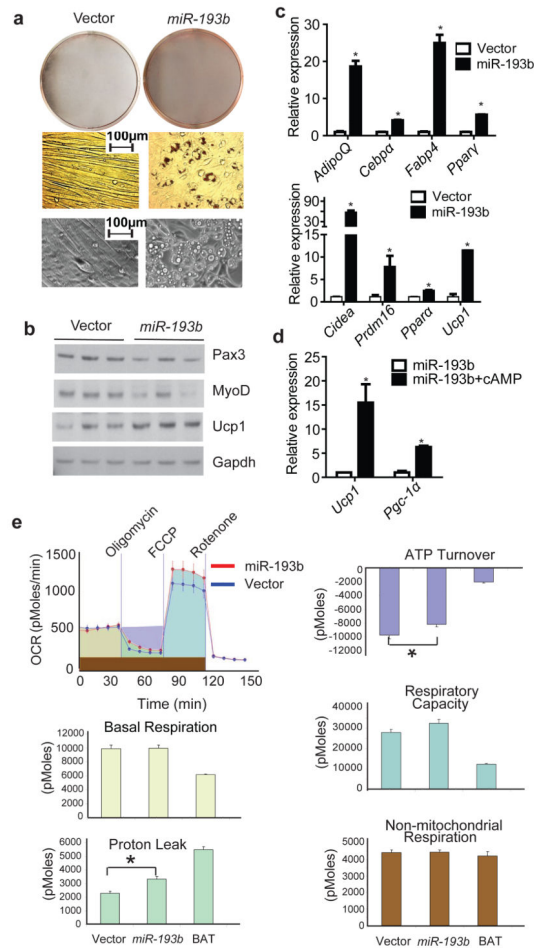


Figure 4. Ectopic expression of *miR-193b* induces C2C12 to form brown adipocytes under adipogenic differentiation conditions

(a), C2C12 cells ectopically expressing *miR-193b* or control were exposed to pro-adipogenic conditions (described in Methods) for 5 days. ORO staining was used to assess lipid accumulation in cells. Representative micrographs of these cells are depicted (bottom row). (b), Western blot for myogenic markers *Pax3*, *MyoD* and brown fat marker *Ucp1*. $n=3$. (c), Real-time PCR analysis for expression of common adipogenesis markers (upper row) and brown fat selective markers (bottom row). $n=3$. (d), C2C12 cells expressing *miR-193b* (day 6) were stimulated with 500 μ M dibutyryl cAMP for 4h, and the expression of thermogenic markers, *Pgc-1 α* and *Ucp1* was examined by real-time PCR. $n=3$. (e), The metabolic profile of C2C12 cells expressing *miR-193b* (day 6) was assessed using the Seahorse XF24 Extracellular Flux Analyzer. A representative curve of the oxygen consumption rates (OCR) of control and *miR-193b* expressing cells at their basal states and upon treatment with drugs used to dissect the multiple components of the respiration process is plotted in the top-left panel. The parameters analyzed are represented by different colors in the upper panel and quantitated in other panels. *In vitro* differentiated primary brown adipocytes (BAT) were used as a reference. $n=8$. * $P < 0.05$, Student's t-test; Means \pm SEM.

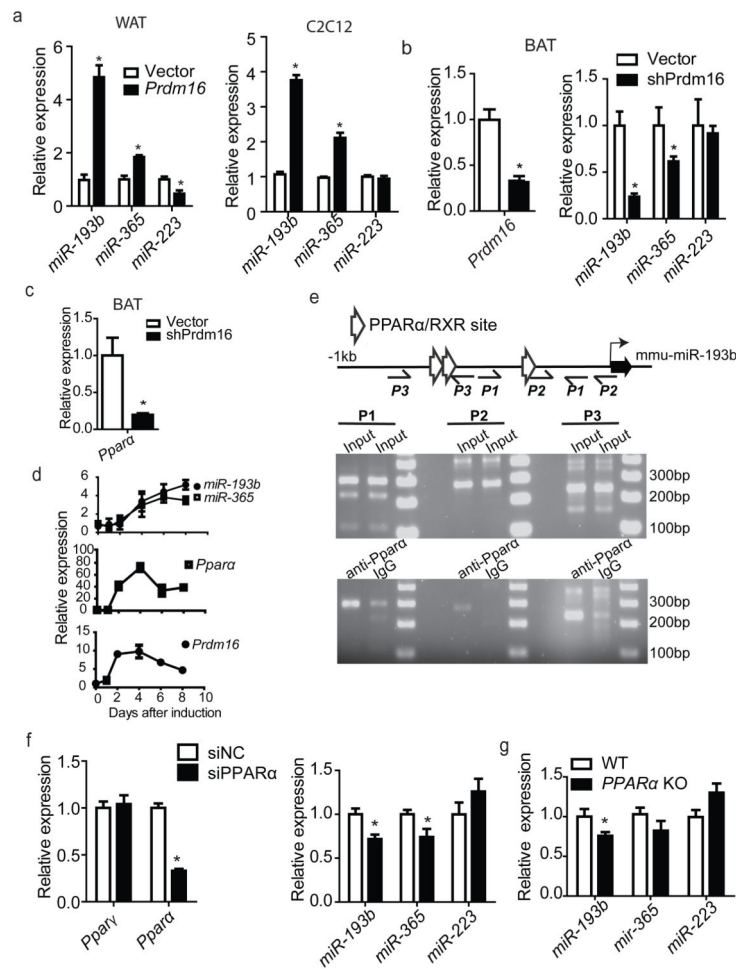


Figure 5. *miR-193b-365* is regulated by *Prdm16*

(a), Subcutaneous white pre-adipocytes (left) and C2C12 myoblasts (right) were infected by retrovirus expressing *Prdm16* two days before differentiation. 5 days after differentiation, real-time PCR were performed to examine the expression of *miR-193b*, *miR-365*, and as a control *miR-223*. $n=3$. (b), Primary brown preadipocytes were infected by retrovirus expressing shRNA targeting *Prdm16* two days before differentiation. By D5 of differentiation, real-time PCR was used to examine the mRNA level of *Prdm16* (left), and *miR-193b*, *miR-365*, and the control *miR-223* (right). $n=3$. (c), Real-time PCR analysis for *Ppara* in primary brown adipocytes retrovirally expressing shRNA for *Prdm16*. (d), Real-time PCR analysis of *miR-193b*, *miR-365*, *Prdm16* and *Ppara* expression levels during adipogenesis of primary brown adipocyte cultures. $n=3$. (e), ChIP analysis for the interaction between *Ppara* and the promoter region of *miR-193b-365*. Immortalized brown adipocyte cultures (Day 5) were fixed and sheared by ultrasonication. Immunoprecipitation was performed with anti-*Ppara* and control IgG. Recovered DNA was amplified by 3 pairs (P1, P2 and P3) of primers designed to span the 1Kb promoter region. Input samples are in the top panel and immunoprecipitated ones in the bottom. (f), Primary brown preadipocytes were transfected with siRNA targeting *Ppara*, and differentiated for 3 days. RT-PCR was performed to examine the expression of *Ppara*, and *miR-193b* and *miR-365*. *Ppar γ* and

miR-223 were used as controls. n=3. (g), RT-PCR was performed to examine the expression of miRNAs in brown adipose tissue isolated from *Ppara* knockout mice (8 week old, Male). Age-matched wild- type mice were used as control. n=6. * $P < 0.05$, Student's t-test; Means \pm SEM.

Author Manuscript

Author Manuscript

Author Manuscript

Author Manuscript